Dynamic relaxation study and experimental verification of dielectric-elastomer minimum-energy structures

S. Siu, L. Rhode-Barbarigos, S. Wagner, and S. Adriaenssens

Citation: Appl. Phys. Lett. **103**, 171906 (2013); doi: 10.1063/1.4826884
View online: http://dx.doi.org/10.1063/1.4826884
View Table of Contents: http://apl.aip.org/resource/1/APPLAB/v103/i17
Published by the AIP Publishing LLC.

Dynamic relaxation study and experimental verification of dielectric-elastomer minimum-energy structures

S. Siu,[1] L. Rhode-Barbarigos,[1,a)] S. Wagner,[2] and S. Adriaenssens[1]
[1]*Form Finding Lab, Department of Civil and Environmental Engineering, Princeton University, Princeton, New Jersey 08544, USA*
[2]*Department of Electrical Engineering, Princeton University, Princeton, New Jersey 08544, USA*

(Received 10 September 2013; accepted 11 October 2013; published online 23 October 2013)

The shape of a dielectric elastomer minimum energy structure (DEMES) depends on the equilibrium between a pre-stretched membrane and an inextensible frame. The authors show that an extended dynamic relaxation method, a technique employed for the form-finding and analysis of pre-stressed structures, can be used to simulate DEMES equilibrium shapes. Physical models show excellent agreement with the shape of computed models. Dynamic relaxation, with its low computational cost, is a powerful form-finding technique that efficiently predicts the equilibrium shape as well as the elastic energy of DEMES. © *2013 AIP Publishing LLC*.
[http://dx.doi.org/10.1063/1.4826884]

Dielectric-elastomer minimum-energy structures (DEMES) are pre-stretched dielectric elastomer membranes[1,2] adhered to thin flexible frames.[3,4] The strain energy of the pre-stretched membrane is transferred to the frame and deforms the system until a strain-energy balance is obtained. The shape of the system thus reflects a local or a global minimum energy state[3,4] that can be varied by applying a voltage. Although DEMES are similar to structures formed by soap films[3] and have stimulated interest throughout disciplines, such as robotics,[4] bioengineering,[5] as well as architecture,[6] they have not yet been investigated using numerical form-finding techniques. Form-finding describes the process of finding a stable equilibrium shape for a system under a specific set of loading, for a set of boundary conditions starting from an arbitrary initial geometry. Here, we show by numerical modeling and experiment that dynamic relaxation (DR), an established form-finding technique extensively employed by architects and structural engineers,[7–11] efficiently simulates realistic DEMES shapes.

In the DR process, a system is modeled as a mesh of links connected with nodes that have masses assigned. Loads are applied to the nodes, while pre-stress is applied in the system through setting an initial link length. The method explores the fact that the static solution for a system subject to loading can be viewed as the equilibrium state of a series of damped vibrations.[12] The governing equation for dynamic relaxation is

$$F_{ext} - F_{int} = M\dot{v} + Dv, \tag{1}$$

where F_{ext} and F_{int} are the external and internal forces at each node, respectively, M corresponds to the nodal mass and D corresponds to damping. Both mass M and damping D are fictitious parameters optimized for the stability and convergence of the method.[13] $\dot{v}$ and v are the acceleration and the velocity at each node, respectively. In this study, kinetic damping is employed to reach static equilibrium as it decreases computational time and improves convergence.[14]

The motion of the system is traced and when a local peak in the total kinetic energy of the system is detected, all velocity components are set to zero. Hence, the damping term Dv in Eq. (1) is abandoned. Expressing the acceleration in finite difference form gives the velocity and the updated geometry for each node

$$v^{t+\Delta t/2} = v^{t-\Delta t/2} + \frac{(F_{ext} - F_{int})}{M}\Delta t, \tag{2}$$

$$x^{t+\Delta t} = x^{t} + v^{t+\Delta t/2}\Delta t, \tag{3}$$

where $v^{t+\Delta t/2}$ and $v^{t-\Delta t/2}$ are the nodal velocities at times $t+\Delta t/2$ and $t-\Delta t/2$, respectively. $x^{t+\Delta t}$ is the nodal position at time $t+\Delta t$ and Δt is the time step applied. The new geometry now obtained allows an update of the internal forces F_{int}. Convergence (equilibrium) is reached when the term $F_{ext} - F_{int}$ is sufficiently small.

DEMES are bending-active systems: their shape is determined by the equilibrium between the pre-stretched membrane and the bending of the initially straight frame. We therefore enhanced the established DR method with clustered and bending elements. Clustered elements are continuous tensile elements that run over frictionless pulleys.[15,16] All links in a clustered element carry the same tensile force. Nodes in clustered elements have fewer kinematic constraints than nodes connected with traditional tensile elements. Bending elements are also composed by a series of links. Moments on the nodes of bending elements are estimated by finite difference modeling of a continuous beam[17,18] and decomposed into shear forces that are added to the existing nodal forces (Eq. (1)).

Here, we analyze a basic DEMES with a rounded triangular shape (Figure 1) and a geometry also studied by O'Brien *et al.*[19] The input for the numerical model includes nodal coordinates and connectivity as well as element characteristics. The values of element characteristics used in the numerical model are given in Table I. Nodes at the base of the system are pinned. Clustered elements are used to model the membrane while bending elements are employed for the frame.

a)Email: landolfr@princeton.edu. Telephone: +1 609 258 5334

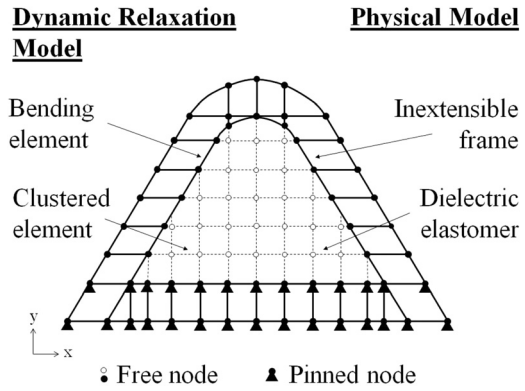

FIG. 1. The DEMES of this study, with designations of the elements of the numerical model at left related to the physical model at right.

Equilibrium shapes are obtained by pre-stretching the clustered elements. To initiate shape changes in the numerical model, its apex is given a small initial deformation. The values of element characteristics used in the numerical model are given in Table I. Figure 2 shows a series of equilibrium shapes obtained when the pre-stretch in the clustered elements is varied.

We made physical models from frames of a 0.127 mm thick acrylonitrile butadiene styrene (ABS) plastic and a dielectric elastomer made of an $h = 0.05$ mm thick 3 M VHB 4905 acrylic adhesive film. The sides of the frame are 52 mm long and 4 mm wide. The side at the base is wider for taping the system to a support plate (Figure 3). The film of Figure 3 was pre-stretched isotropically to 200% of its initial length before it was adhered to the frame. Not shown in Figure 3 are the conducting carbon grease electrodes that were spread over both faces of the elastomer. The completed system is voltage-actuated from an EMCO ultra-miniature DC to HV DC converter. The shape of the physical model of Figure 3 reflects the initial balance between the pre-stretched membrane and the inextensible frame. When voltage is applied the membrane expands, and a sufficiently high voltage makes the whole system flat.

Figure 3 shows the shape of a physical model and the equilibrium shape obtained with the dynamic relaxation DEMES model. The shape of the DR model results from the application of pre-stretch in clustered elements of a flat system (Figure 1) and is similar to the shape of the physical model. However, the equilibrium shape of the physical model and the numerical model (Figure 3) correspond to different pre-stretch states. The membrane in the physical model was pre-stretched at 200% of its initial length, while in the numerical model a similar shape is obtained at 150%. This discrepancy is most likely due to inaccuracies in the physical properties employed in the numerical model.[20] Another source of discrepancy is hysteresis in the physical DEMES system,[21] which is not accounted for in the numerical model.

TABLE I. Values for element characteristics used in the numerical model.

Element type	Characteristic	Value
Clustered elements	Elastic modulus	1 N/mm^2
	Cross-sectional area	0.08 mm^2
Bending elements	Elastic modulus	2600 N/mm^2
	Cross-sectional area	0.5 mm^2
	Second moment of area	0.0003 mm^4

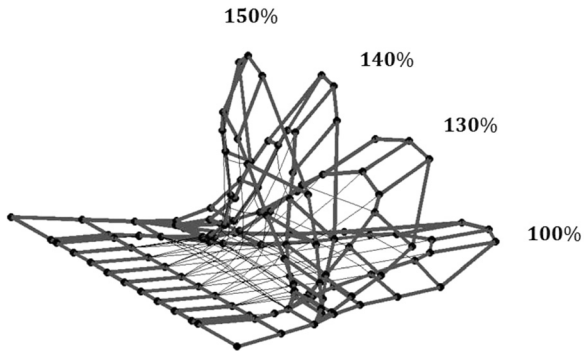

FIG. 2. Equilibrium shapes for four different pre-stretch states (% pre-stretch of the membrane).

Figure 4 shows the stroke (bending angle at a voltage V minus the bending angle at $V = 0$) in function of applied voltage V for three different DEMES physical samples. Note that at $V = 0$ the system is bent the most. Increasing V compresses the membrane and thereby increases the stroke. The curves differ slightly because of irregularities in fabrication. All three samples show substantial change of shape at $V \cong 1$ kV and become flat at V $\cong 2.25$ kV.

To obtain a better understanding of the DEMES equilibrium states, we calculated the energies for the physical and the DR (numerical) model. The energy in the physical model is calculated as the energy of a charged capacitor

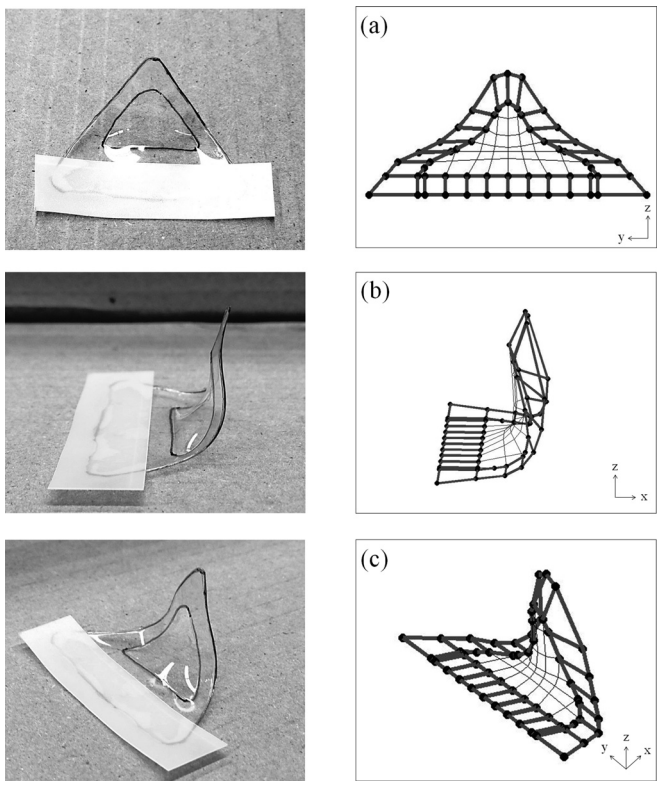

FIG. 3. At left, three views of a DEMES system in its initial state, before application of carbon electrodes. At right, the DEMES equilibrium shape obtained with dynamic relaxation: (a) top, (b) side, and (c) perspective.

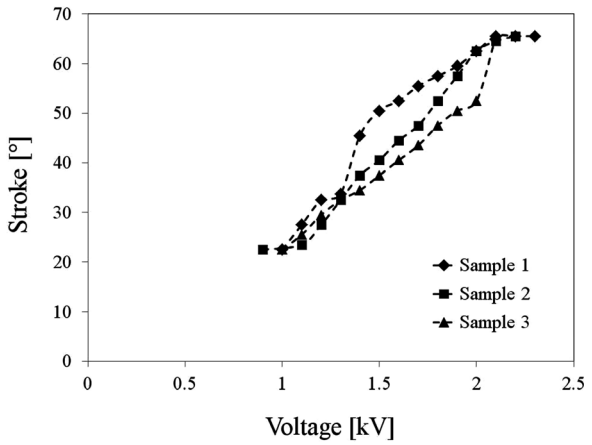

FIG. 4. DEMES actuation: stroke vs. applied voltage V for three physical samples.

$E_{cap} = A\,CV^2/2$. We use average values of the voltage V, A is the area of the membrane, and C is its capacitance per unit area (with the thickness h of the membrane in its stretched state) and the dielectric constant is 4.65.[2,20] In the dynamic relaxation model, the energy $E_{DR} = \sum(N\varepsilon L/2) + \sum(M^2L/2EI)$ corresponds to the sum of strain energies in the clustered and bending elements for each bending state, where N and M are the axial force and the bending moment, respectively. L is the length of an element, E is its elastic modulus, and I is the second moment of area. ε is the axial strain. Figure 5 relates E_{cap} and E_{DR} to the stroke. The numerical model requires more energy for actuation than the physical model. The difference may be due to fabrication tolerances and uncertainties in material properties (assumptions made for the energy estimations such as the value taken for the dielectric constant[2,20]). In both the numerical and the physical models, the elastomer dominates energy storage at low strokes. The large discrepancy at high strokes most likely results from the different geometries of the frame in the two models. While in the numerical model the frame suddenly begins to dominate energy storage, in the physical model the frame takes over gradually. Both the physical and the numerical models begin to rise rapidly at stroke values of 140° and 120°, respectively. At this rise, the system reaches a physical boundary: its maximum bent configuration, where further pre-stretching of the membrane has a small or no effect on the frame.

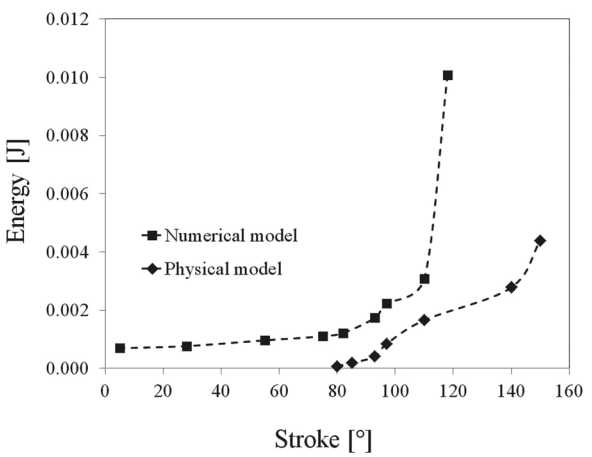

FIG. 5. Energy for the physical and the numerical model for different stroke values.

We conclude that the dynamic relaxation technique originally developed for structural form-finding can predict realistic equilibrium shapes and elastic energies of future DEMES applications[22] at much lower computational cost than existing numerical models.[23,24] These models come with high computational cost because of complex analytical and strain-energy formulations in finite element methods.[19,25,26] Our DR algorithm for the design of shape-shifting DEMES applications enables the efficient exploration of large design spaces. To validate the method, we studied a specific DEMES system numerically and experimentally. DR is found to correctly predict the DEMES equilibrium shape within a margin given by experimental inaccuracies, without the computational cost of currently available methods.

We thank Maggie Zhang and Professor Qibing Pei of UCLA for their valuable experimental advice.

[1]R. Pelrine, R. D. Kornbluh, and J. P. Joseph, Sens. Actuators, A **64**, 77–85 (1998).
[2]R. Pelrine, R. D. Kornbluh, J. Eckerle, P. Jeuck, S. Oh, Q. Pei, and S. Stanford, Proc. SPIE **4329**, 148–156 (2001).
[3]G. Kofod, M. Paajanen, and S. Bauer, Appl. Phys. A **85**, 141–143 (2006).
[4]M. T. Petralia and R. J. Wood, in *2010 IEEE/RSJ International Conference on Intelligent Robots and Systems (IROS)* (2010), pp. 2357–2363.
[5]B. O'Brien, T. Gisby, E. Calius, S. Xie, and I. Anderson, Proc. SPIE **7287**, 728706 (2009).
[6]U. Berardi, Intell. Build. Int. **2**, 167–178 (2010).
[7]M. R. Barnes, Int. J. Space Struct. **14**, 89–104 (1999).
[8]K. Hincz, Int. J. Space Struct. **24**, 143–152 (2009).
[9]P. D. Gosling and W. J. Lewis, Comput. Struct. **61**, 885–895 (1996).
[10]J. Rodriguez, G. Rio, J. M. Cadou, and J. Troufflard, Thin-Walled Struct. **49**, 1468–1474 (2011).
[11]L. Rhode-Barbarigos, N. Bel Hadj Ali, R. Motro, and I. F. C. Smith, Int. J. Space Struct. **27**, 81–96 (2012).
[12]A. S. Day, Engineer **219**, 218–221 (1965).
[13]T. B. Belytschko and T. J. R. Hugues, *Computational Methods for Transient Analysis: Computational Methods in Mechanics; Mechanics and Mathematical Methods*, Series of Handbooks (North-Holland, Amsterdam, New York, 1983).
[14]P. A. Cundall, "Numerical methods in engineering," in *Proceedings of the EF Conference on Numerical Methods in Geomechanics* (1976), Vol. 1, pp. 132–150.
[15]K. W. Moored and H. Bart-Smith, Int. J. Solids Struct. **46**, 3272–3281 (2009).
[16]N. Bel Hadj Ali, L. Rhode-Barbarigos, and I. F. C. Smith, Int. J. Solids Struct. **48**, 637–647 (2011).
[17]S. Adriaenssens and M. R. Barnes, Eng. Struct. **23**, 29–36 (2001).
[18]M. R. Barnes, S. Adriaenssens, and M. Krupka, Comput. Struct. **119**, 60–67 (2013).
[19]B. O'Brien, E. Calius, S. Xie, and I. Anderson, Proc. SPIE **6927**, 69270T (2008).
[20]T. G. McKay, E. Calius, and I. A. Anderson, Proc. SPIE **7287**, 72870P (2009).
[21]X. Zhao, W. Hong, and Z. Suo, Phys. Rev. B **76**, 134113 (2007).
[22]N. M. Wereley and J. M. Sater, *Plants and Mechanical Motion: A Synthetic Approach to Nastic Materials and Structures* (Destech Publications Incorporated, Lancaster, PA, 2012).
[23]N. Goulbourne, E. Mockensturm, and M. Frecker, J. Appl. Mech. **72**, 899–906 (2005).
[24]G. Kofod, W. Wirges, M. Paajanen, and S. Bauer, Appl. Phys. Lett. **90**, 081916 (2007).
[25]X. Zhao and Z. Suo, Appl. Phys. Lett. **93**, 251902 (2008).
[26]W. Hong, J. Mech. Phys. Solids **59**, 637–650 (2011).